Apolipoprotein CIII links islet insulin resistance to β-cell failure in diabetes

Karin Åvall[a,1], Yusuf Ali[a,b,1], Ingo B. Leibiger[a], Barbara Leibiger[a], Tilo Moede[a], Meike Paschen[a], Andrea Dicker[a], Elisabetta Daré[a], Martin Köhler[a], Erwin Ilegems[a], Midhat H. Abdulreda[c], Mark Graham[d], Rosanne M. Crooke[d], Vanessa S. Y. Tay[b], Essam Refai[a], Stefan K. Nilsson[e], Stefan Jacob[a], Lars Selander[a], Per-Olof Berggren[a,b,c,2], and Lisa Juntti-Berggren[a,2]

[a]The Rolf Luft Research Center for Diabetes and Endocrinology, Karolinska Institutet, Karolinska University Hospital L1, SE-171 76 Stockholm, Sweden; [b]Lee Kong Chian School of Medicine, Nanyang Technological University, Singapore 637 553; [c]Diabetes Research Institute, Department of Surgery, University of Miami, Miller School of Medicine, Miami, FL 33136; [d]Isis Pharmaceuticals, Carlsbad, CA 92010; and [e]Department of Medical Biosciences, Unit of Physiological Chemistry 6M, Umeå University, SE-901 85 Umeå, Sweden

Edited by Solomon H. Snyder, Johns Hopkins University School of Medicine, Baltimore, MD, and approved April 14, 2015 (received for review December 12, 2014)

Insulin resistance and β-cell failure are the major defects in type 2 diabetes mellitus. However, the molecular mechanisms linking these two defects remain unknown. Elevated levels of apolipoprotein CIII (apoCIII) are associated not only with insulin resistance but also with cardiovascular disorders and inflammation. We now demonstrate that local apoCIII production is connected to pancreatic islet insulin resistance and β-cell failure. An increase in islet apoCIII causes promotion of a local inflammatory milieu, increased mitochondrial metabolism, deranged regulation of β-cell cytoplasmic free Ca^{2+} concentration ($[Ca^{2+}]_i$) and apoptosis. Decreasing apoCIII in vivo results in improved glucose tolerance, and pancreatic apoCIII knockout islets transplanted into diabetic mice, with high systemic levels of the apolipoprotein, demonstrate a normal $[Ca^{2+}]_i$ response pattern and no hallmarks of inflammation. Hence, under conditions of islet insulin resistance, locally produced apoCIII is an important diabetogenic factor involved in impairment of β-cell function and may thus constitute a novel target for the treatment of type 2 diabetes mellitus.

diabetes | apoCIII | insulin resistance | pancreatic islets

Glucose homeostasis in mammals is tightly controlled by a balance between peripheral tissue insulin sensitivity with corresponding glucose uptake and regulated insulin secretion by pancreatic β cells. If this balance is disturbed, diabetes develops. The progression of type 2 diabetes mellitus (T2DM) occurs in phases. The initial phase is characterized by peripheral tissue insulin resistance with a β-cell compensatory response of increasing mass and insulin secretion. With prolonged hyperinsulinemia, however, β cells start to fail, causing defects in insulin secretion and eventually increased β-cell apoptosis (1, 2). Although being crucial for the development of novel diabetes therapies, the direct link between insulin resistance and β-cell failure in T2DM is still not known.

Apolipoprotein CIII (apoCIII) resides on apoB lipoproteins and high-density lipoproteins and regulates their metabolism by inhibiting lipoprotein lipase (3, 4). The expression of apoCIII is increased by insulin deficiency and insulin resistance (5, 6), and recently it has been shown that hyperglycemia induces apoCIII transcription (7). On top of high levels of circulating triglycerides, mice overexpressing apoCIII are more susceptible to high-fat diet (HFD)-induced diabetes (8). In humans, elevated levels of circulating apoCIII are associated with a number of adverse effects, including cardiovascular problems, inflammation, and insulin resistance (9, 10). Conversely, humans with a lifelong reduction of the apolipoprotein, due to mutations in the apoCIII gene, benefit from a favorable pattern of lipoproteins, increased insulin sensitivity and longevity, lower incidence of hypertension, and protection against cardiovascular diseases (11–13).

We now show that apoCIII serves as a link between insulin resistance and β-cell failure in T2DM. The mechanistic explanation is that specific insulin resistance within the pancreatic islet leads to local expression of apoCIII, resulting in an autocrine negative feedback loop for β-cell function and survival.

Results

Insulin Signaling in Ob/Ob Islets. The obese/obese (ob/ob) mouse is known to progressively develop insulin resistance and a transient hyperglycemia (14). Using this mouse model at the age of 4–12 wk, we found that blood glucose and body weight increased progressively (Fig. 1 *A* and *B*) and that nonfasting insulin levels remained unchanged higher than in control animals (Fig. 1*C*). We determined the mRNA expression levels of glucokinase (*gck*), insulin-receptor substrate 1 (*irs1*), insulin-receptor substrate 2 (*irs2*), vesicle-associated membrane protein 2 (*vamp2*), synaptosomal-associated protein 25 (*snap25*), and ras-related protein 27a (*rab27a*), genes that have been demonstrated to be controlled by insulin receptor (IR)-activated phosphatidylinositol 3-kinase (PI3K) activity (15, 16). All genes were down-regulated in 12-wk-old

Significance

Insulin resistance and β-cell failure are the major defects in type 2 diabetes. We now demonstrate that local insulin resistance-induced increase in apolipoprotein CIII (apoCIII) within pancreatic islets causes promotion of an intraislet inflammatory milieu, increased mitochondrial metabolism, deranged regulation of β-cell cytoplasmic free Ca^{2+} concentration ($[Ca^{2+}]_i$), and apoptosis. Decreasing apoCIII in vivo in animals with insulin resistance improves glucose tolerance, and apoCIII knockout islets transplanted into diabetic mice, with high systemic levels of apoCIII, demonstrate a normal $[Ca^{2+}]_i$ response pattern and no hallmarks of inflammation. Hence, under conditions of islet insulin resistance, locally produced apoCIII is an important diabetogenic factor involved in impairment of β-cell function and may thus constitute a novel target for the treatment of type 2 diabetes.

Author contributions: K.Å., Y.A., I.B.L., B.L., P.-O.B., and L.J.-B. designed research; K.Å., Y.A., I.B.L., B.L., T.M., M.P., A.D., E.D., M.K., E.I., V.S.Y.T., E.R., S.J., and L.S. performed research; M.G., R.M.C., and S.K.N. contributed new reagents/analytic tools; K.Å., Y.A., I.B.L., B.L., T.M., M.P., E.D., M.K., E.I., M.H.A., P.-O.B., and L.J.-B. analyzed data; and Y.A., I.B.L., P.-O.B., and L.J.-B. wrote the paper.

Conflict of interest statement: P.-O.B. is cofounder and CEO of Biocrine, a biotech company, and M.H.A., I.B.L., B.L., M.K., and E.I. are serving as consultants for Biocrine. M.G. and R.M.C. are employees of Isis Pharmaceuticals, Inc.

This article is a PNAS Direct Submission.

[1]K.Å. and Y.A. contributed equally to this work.

[2]To whom correspondence may be addressed. Email: lisa.juntti-berggren@ki.se or Per-Olof.Berggren@ki.se.

This article contains supporting information online at www.pnas.org/lookup/suppl/doi:10.1073/pnas.1423849112/-/DCSupplemental.

ob/ob islets (Fig. 1*D*). This is consistent with previous findings where a significantly reduced PI3K activity was found in islets from ob/ob mice at 12 wk of age compared with islets from age-matched ob/lean littermates (17, 18).

Progressive Change in FoxO1-Regulated Gene Expression in Ob/Ob Islets Over Time. One of the ways in which insulin induces changes in gene expression is through the phosphorylation cascade of Akt and its downstream target forkhead transcription factor FoxO1. Insulin-mediated activation of Akt leads to phosphorylation of FoxO1 with its nuclear exclusion and loss of transcriptional activity. This signaling cascade has been shown to be crucial in maintaining β-cell function and proliferation during either insulin resistance or insult/injury (19–21). We determined levels of phospho-Akt and phospho-FoxO1 in ob/ob islets. There was a significant reduction in phospho-Akt (Ser473) and phospho-FoxO1 (Ser256) in islets from 12-wk-old ob/ob mice compared with islets from 4-wk-old ob/ob mice (Fig. 1*E*). Total Akt protein levels within these islets were not significantly different across time. Total FoxO1 protein levels in the islet could not be successfully measured because of poor signal from immunoblots, reflecting low expression of FoxO1. To circumvent this, we determined mRNA levels of FoxO1 and found no significant difference in all of the age groups studied (Fig. 1*E*). The levels of nuclear FoxO1 were higher in islets from 12-wk-old ob/ob mice compared with islets from ob/lean. This was shown both in vivo, using the anterior chamber of the eye (ACE) transplantation technique (22) (Fig. 1*F*), and in vitro (Fig. 1 *G* and *H*). Hence, the simultaneous reduction of phospho-FoxO1 and increase in nuclear FoxO1 further corroborates the above described changes in ob/ob islet gene expression, as *irs1*, *irs2*, *vamp2*, and *rab27a* have been suggested to be repressed by FoxO1 (15).

IR-mediated repression of FoxO1 is pivotal in maintaining the balance between carbohydrate and fat metabolism in hepatocytes (3). In insulin-resistant hepatocytes, reduced FoxO1 phosphorylation, and hence its activation as a transcription factor, promotes the expression of apoCIII, a modulator of circulating triglycerides; glucose-6-phosphatase, a key gluconeogenic enzyme; and mttp1, a microsomal triglyceride transfer protein that is involved in lipoprotein assembly (23). To explore if a similar mechanism occurs in ob/ob islets with declining levels of phospho-FoxO1, we determined the mRNA expression levels of the FoxO1 target genes *apoCIII*, *g6pc2* (islet-specific glucose-6-phosphatase), and *mttp1*. There was a significant increase in ob/ob islet mRNA expression of all three genes across time (Fig. 2*A* and Fig. S1 *A* and *B*). Together, these data suggest that insulin resistance at the islet level leads to a change in the expression of genes that are positively or negatively regulated by FoxO1. Of these, apoCIII expression stands out as an islet factor observed in both α and β cells (Fig. 2*A* and Fig. S1*C*). This is an important finding, as this apolipoprotein is known to be involved in both β-cell dysfunction (24) and type 1 diabetes mellitus (25, 26).

ApoCIII Is Increased in Islets and Serum in Diabetes, and Systemically Decreasing It in Vivo Improves the Diabetic Phenotype. As there was a threefold increase in apoCIII mRNA levels in islets from 12-wk-old ob/ob mice, without any difference in liver and intestine apoCIII expression (Fig. 2 *A*–*C*), we decided to determine the systemic levels of apoCIII. The immunoblots showed increased apoCIII levels in serum of ob/ob mice (Fig. S2 *A* and *B*). Given that liver is the main source of apoCIII, the higher levels of circulating apoCIII cannot be explained by the enhanced islet release of the apolipoprotein but rather reflects reduced cellular uptake of triglyceride-rich (VLDL) remnants, similar to what has been previously reported (27).

To explore the effects of decreasing apoCIII in vivo, ob/ob mice were treated with antisense oligonucleotides specific for apoCIII or an inactive control. These antisense oligonucleotides decrease apoCIII by more than 50% (Fig. 2*D*). The lowering of apoCIII led to a reduced body weight and, most importantly, an improved glucose tolerance (Fig. 2 *E* and *F*). Immunostaining of islets from two healthy human subjects (Fig. S3 *1* and *2*) and one T2DM patient (Fig. S3 *3*) showed a higher degree of apoCIII-positive cells in the T2DM islets, which is in accordance with the findings in the ob/ob mice. It should be noted that not all insulin-containing cells are apoCIII positive. This most likely indicates that at the time when these islets were harvested, not all β cells in the islets of this patient were insulin resistant. Furthermore, we observed that there are apoCIII-positive cells that do not contain insulin, which is in accordance with our results from sorted islet cells (Fig. S1*C*).

ApoCIII Overexpression Increases $[Ca^{2+}]_i$ in MIN6 Cells. To corroborate the negative role of locally produced apoCIII on β-cell function, this apolipoprotein was overexpressed in the insulin-secreting cell line MIN6. Hampered by the ability of an antibody to recognize apoCIII in mouse liver sections and lysates, we resorted to a c-Myc–tagged mouse apoCIII construct that allowed us to explore the localization of Myc-apoCIII within β cells. Myc-apoCIII was detectable in media of the Myc-apoCIII–transfected cells after a 24-h culture period, indicating that the synthesized apoCIII is being readily released into the extracellular medium (Fig. 3*A*). No colocalization between Myc-apoCIII and insulin C-peptide could be detected in the transfected cells (Fig. 3*B*). MIN6 cells transfected with either Myc-apoCIII or a control vector were loaded with fura-2 acetoxymethyl ester (Fura-2AM) to determine the effect of mouse apoCIII on $[Ca^{2+}]_i$ upon maximum activation of the voltage-gated Ca^{2+} channels by KCl stimulation. A significantly higher increase in $[Ca^{2+}]_i$, after KCl exposure, was observed in MIN6 cells expressing Myc-apoCIII compared with the control transfected cells (Fig. 3*C*). Compared with control, a higher increase in $[Ca^{2+}]_i$ was also seen in nearby nontransfected cells in the same culture dish upon depolarization. Hence, it is likely that in addition to the autocrine effect on the transfected cell itself, apoCIII may exert a paracrine effect on other islet cells.

Reduced Endogenous Islet ApoCIII in Vitro and in Vivo Results in Improved $[Ca^{2+}]_i$ Handling and Less Apoptosis. Next, we investigated how a specific lowering of apoCIII in the islet affected function and survival of the β cells, here depicted as changes in $[Ca^{2+}]_i$ and apoptosis. Expression of apoCIII in islets exposed to antisense oligonucleotides was 20% compared with control islets (Fig. 4*A*). Islets were loaded with Fura-2AM to determine the effect of apoCIII on $[Ca^{2+}]_i$, subsequent to both high glucose and KCl exposure. As previously noted (18), ob/ob islets had a significantly higher peak amplitude of $[Ca^{2+}]_i$ compared with ob/lean islets (Fig. 4*B*). The peak amplitude of $[Ca^{2+}]_i$, upon stimulation with either glucose or KCl, was reduced in ob/ob islets where apoCIII had been lowered (Fig. 4 *B* and *C*).

Although ob/ob islets are hyperplastic with massive β-cell proliferation, it does not rule out the presence of apoptosis in these islets. We determined the level of apoptosis in freshly isolated islets by measuring the activity of caspase 3/7. Apoptosis in islets from 12-wk-old ob/ob mice was significantly higher compared with islets from 4-wk-old ob/ob mice (Fig. 4*D*). This is consistent with a previous finding where reduced levels of phospho-FoxO1 in islets of New Zealand obese mice resulted in higher levels of apoptosis (28). Lowering endogenous apoCIII in islets from 12-wk-old ob/ob mice, when apoCIII levels are the highest, decreased caspase 3/7 activity by 31%, compared with islets treated with scrambled antisense (Fig. 4 *E*, *Right*). Because our previous results have shown that apoCIII increases the activity of the voltage-gated Ca^{2+} channel (29) and caspase 3/7 activity is driven by Ca^{2+}, we exposed β cells to the Ca^{2+}-channel blocker verapamil, and this reduced caspase activity by 15% (Fig. 4 *E*, *Left*). Together, these results suggest that increased FoxO1-induced

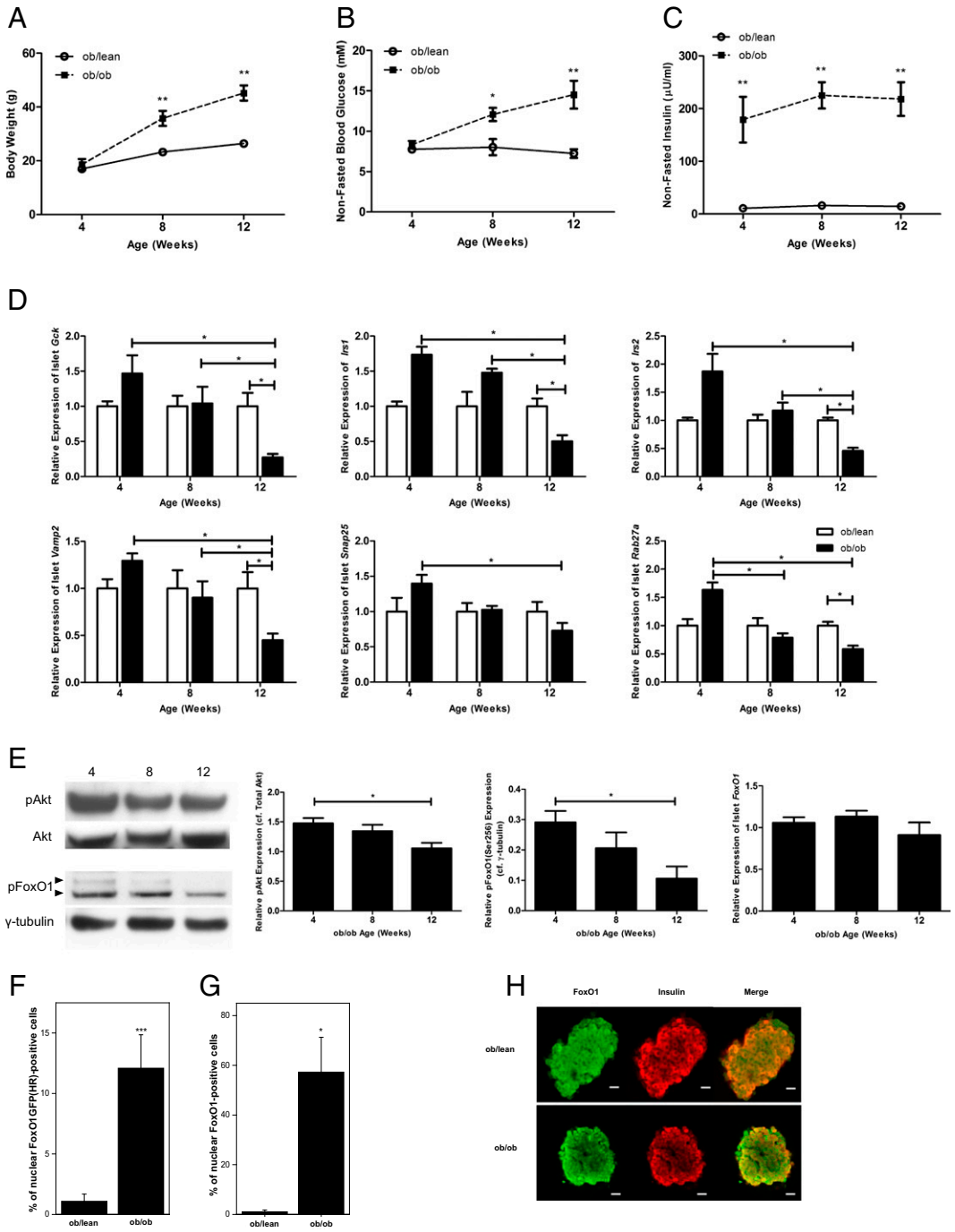

Fig. 1. Exacerbated hyperglycemia and reduced insulin signaling in ob/ob islets across time. (*A*) Average body weight, (*B*) nonfasted blood glucose levels, and (*C*) nonfasted plasma insulin levels measured in both ob/ob and age-matched ob/lean mice at 4, 8, and 12 wk of age ($n = 8$–11). (*D*) Pancreatic islet gene expression changes between obese and lean controls at 4, 8, and 12 wk of age. mRNA levels were determined by real-time qPCR, normalized to β-actin. Expression levels of ob/ob were compared with those of ob/lean, which were set at 1.0. There was no significant change in ob/lean gene expression over time ($n = 4$–9). (*E*) Western blot analysis of ob/ob islet lysates prepared from animals at 4, 8, and 12 wk of age, probed with antibodies specific for pAkt, total Akt, pFoxO1, and γ-tubulin. Bands were quantitated by densitometry. Total FoxO1 immunoblots had poor signal-to-noise ratios, and thus mRNA levels of FoxO1 were measured instead ($n = 3$–4). (*F*) In vivo distribution of FoxO1 in islets from 12-wk-old ob/lean and ob/ob mice transplanted into the ACE of syngeneic mice ($n = 13$). (*G*) Freshly isolated islets from 12-wk-old ob/lean and ob/ob mice were immunostained for FoxO1 and insulin, and the percentage of FoxO1-positive cells was determined ($n = 3$). (*H*) Representative maximum projection of ob/lean and ob/ob islets ($n = 10$). FoxO1 is labeled with Alexa488, and green is used as a digital pseudocolor for fluorescence emitted from Alexa488; red is used as a digital pseudocolor for fluorescence emitted from Alexa633, representing insulin. Yellow obtained after overlaying the Alexa488 and Alexa633 signals indicates colocalization. (Scale bar, 30 μM.) Data are presented as mean ± SEM. $^*P < 0.05$, $^{**}P < 0.01$, $^{***}P < 0.001$ by student's *t* test or ANOVA (Tukey's post hoc).

expression of apoCIII within the ob/ob pancreatic islet leads to deranged $[Ca^{2+}]_i$ and an increase in β-cell apoptosis.

Because liver is the predominant source of apoCIII, it is necessary to clarify the extent to which an increased local production

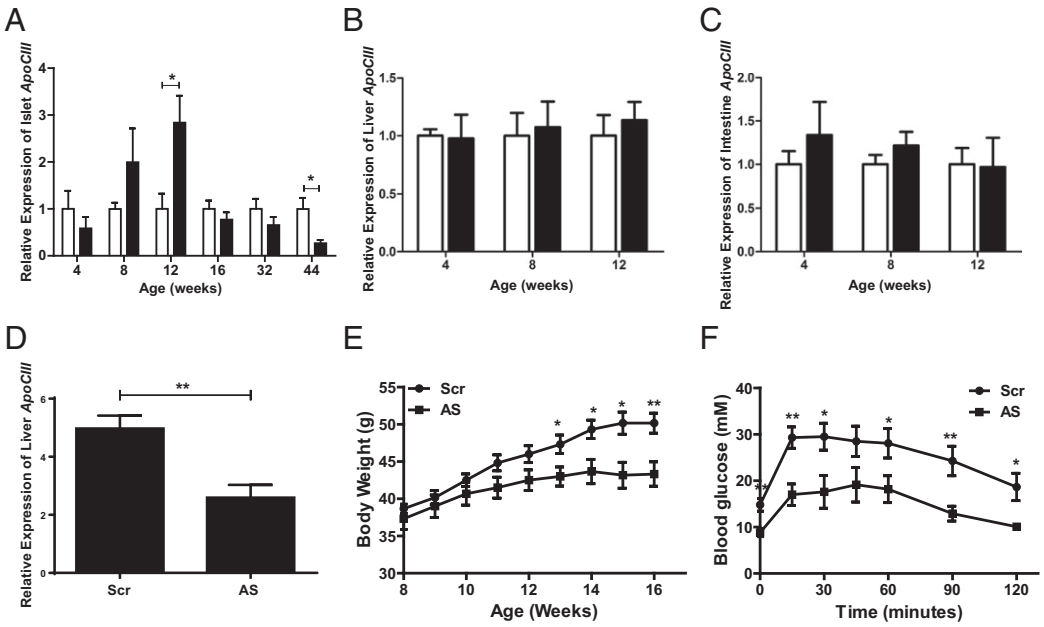

Fig. 2. Expression of apoCIII in islets, liver, and small intestine across time and the in vivo effects of decreasing apoCIII in the ob/ob mouse. (*A*) Pancreatic islet, (*B*) liver, and (*C*) small intestine apoCIII gene expression was compared between obese and lean controls at 4, 8, 12, 16, 32, and 44 wk of age (*A*) and 4, 8, and 12 wk (*B* and *C*). mRNA levels were determined by real-time qPCR, normalized to β-actin (n = 4–8, 5–7, 5–8, 4, 4–5, and 4, respectively). (*D*) Liver mRNA levels of apoCIII after antisense treatment (n = 6). (*E*) Body weight in ob/ob mice treated with scrambled (Src, squares) or apoCIII-specific (AS, circles) antisense (n = 6). (*F*) IPGTT after 8 wk of antisense treatment (n = 6). Data are presented as mean ± SEM. $^*P < 0.05$, $^{**}P < 0.01$.

of the apolipoprotein within the islet will have an effect on the β cell on top of that already provided by the liver. For this purpose, we took the advantage of a global apoCIII$^{-/-}$ mouse (30) and the ACE as an in vivo experimental platform (22). By transplanting islets from either knockout or ob/ob mice into the eye of ob/ob mice with high serum levels of apoCIII, we created an in vivo model where both grafts were subjected to high systemic levels of the apolipoprotein, but only the ob/ob islets maintained a local production of apoCIII (Fig. 5*A*). The islets were allowed to be in the eye for 2 wk, and during this time, they developed a normal vascularization and hence were exposed to high systemic levels of apoCIII (Fig. 5*B*). Thereafter the islets were dissected out of the eye and subjected to measurements of $[Ca^{2+}]_i$ subsequent to depolarization with KCl, to maximally activate the voltage-gated Ca^{2+} channels. Islets from the apoCIII$^{-/-}$ mice demonstrated a lower increase in $[Ca^{2+}]_i$, suggesting that the local islet production of apoCIII indeed has a detrimental effect on β-cell $[Ca^{2+}]_i$ handling (Fig. 5 *C* and *D*).

To further substantiate the significance of intraislet levels of apoCIII for pancreatic β-cell function and survival, islets from apoCIII$^{-/-}$ mice and C57BL/6 (B6) mice, as the control, were transplanted into the eyes of B6 mice. Islets from apoCIII$^{-/-}$ mice were transplanted into the right eye, and control islets from B6 mice were transplanted into the left eye of the same recipient mouse (Fig. 6*A*). The islets were allowed to be vascularized, and thereafter the transplanted mice were fed a HFD until they showed an impaired glucose tolerance. ApoCIII levels, determined in serum and islets, were increased in B6 mice on HFD compared with mice fed normal chow (Fig. 6 *B* and *C*). In this unique experimental setup, the very same animal served both as a control and an islet cell-specific apoCIII knockout. It was thus possible to expose the two types of islets to exactly the same high systemic serum levels of apoCIII, originating from the liver, and the only difference was that the islets in the right eye were not expressing apoCIII, whereas those in the left eye did. The islets were imaged over time from 1 to 3 mo posttransplantation (Fig. 6*D*). As expected, the islets from the control B6 mice increased in size with time. In contrast, the apoCIII$^{-/-}$ islets had a smaller increase in size compared with the control islets, despite being exposed to the same high systemic levels of apoCIII (Fig. 6 *D* and *E*). Importantly, vessel density, number of macrophages, and NAD(P)H:FAD ratio were lower in the transplanted apoCIII$^{-/-}$ islets (Fig. 6 *F*–*J*), suggesting that the lack of intraislet apoCIII production prevents the HFD-induced inflammatory reaction. The difference in size between B6 and apoCIII$^{-/-}$ islets is likely to be the consequence of a local apoCIII-induced inflammatory milieu due to islet insulin resistance and thereby more vessels and an increased compensatory β-cell proliferation (Fig. S4). In parallel, local islet production of apoCIII leads to changed metabolism, deranged Ca^{2+} handling, and activation of caspase 3/7, all negative effects on β-cell function and survival that can be prevented by blocking/lowering apoCIII or by blocking Ca^{2+} influx through voltage-gated Ca^{2+} channels.

Discussion

Diabetes is a severe, multifactorial, and lifelong disease, spreading like an epidemic worldwide, where available treatment strategies are inadequate. T2DM is characterized by two major defects—namely, insulin resistance and β-cell failure—although the link between the two is not clear. In the present study, we report on apoCIII as a tentative factor linking insulin resistance to β-cell failure in T2DM. The mechanistic explanation is that islet insulin resistance can promote local apoCIII production that negatively affects function and survival of the pancreatic β cell, on top of the already high levels of the apolipoprotein promoted by the liver. There could also be a contribution by the hyperglycemia, as this has been shown to induce apoCIII gene expression in hepatocytes (7).This points to much wider negative effects of apoCIII in the pathogenesis of diabetes than previously assessed from cardiovascular studies.

T2DM develops as a consequence of the pancreatic β cell no longer being able to cope with increased insulin resistance in the peripheral insulin target tissues, like the liver (31). We and others have previously shown that also the pancreatic β cell is

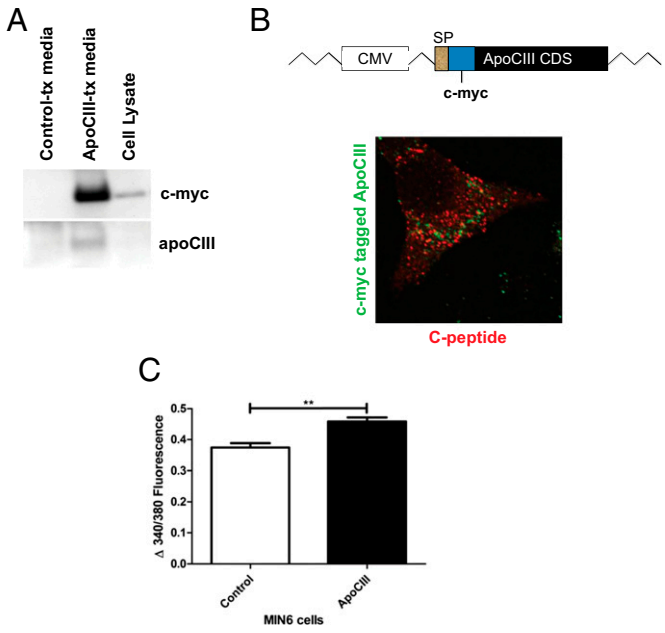

Fig. 3. Overexpressing Myc-apoCIII in Min6 cells affects Ca^{2+} handling. (*A*) Myc-apoCIII was detectable in media of the Myc-apoCIII–transfected cells after a 24-h culture period. (*B*) There was no colocalization of Myc-apoCIII and insulin C-peptide in the transfected cells. (*C*) Both Myc-apoCIII– and control-transfected Min6 cells were loaded with Fura-2AM to determine $[Ca^{2+}]_i$ upon membrane depolarization using 25 mM KCl ($n = 3$–4). Data are presented as mean ± SEM. $^{**}P < 0.01$ by student's *t* test.

equipped with IRs and thereby applies insulin-induced signal transduction for function and survival (16). Importantly, we now demonstrate that the pancreatic islet can be subjected to insulin resistance, leading to a progressive change in FoxO1-regulated gene expression in ob/ob islets over time. Hence, with prolonged hyperinsulinemia, insulin signaling at the islet level was compromised, similar to what has been reported for the β-cell–specific IR knockout mouse (βIRKO) and the β-cell–specific PI3K subunit p85α knockout mouse (βPik3r1) (15, 32). In diabetic ob/ob mice, there is therefore not only insulin resistance in the peripheral target tissues, leading to increased serum levels of apoCIII, but also islet insulin resistance, resulting in increased local production of the apolipoprotein. Interestingly, we also found an increased number of apoCIII-positive cells in islets from a patient with T2DM compared with islets from healthy individuals. In line with the overall negative effects reported for apoCIII (9, 10), our findings that systemically decreasing the levels of this apolipoprotein in vivo improves the diabetic phenotype are logical.

To clarify, at the molecular level, how local islet production of apoCIII affected the β cell, we took advantage of MIN6 cells overexpressing the apolipoprotein. Interestingly, these cells released apoCIII, which promoted both autocrine and paracrine Ca^{2+} influx. This is consistent with previously observed effects of exogenously added human apoCIII on both rat insulinoma cells (26) and primary mouse β cells (33). Next we investigated how a specific lowering of apoCIII in the islet affected β-cell $[Ca^{2+}]_i$ and apoptosis. Subsequent to antisense treatment, stimulated $[Ca^{2+}]_i$ increase was reduced. This effect on $[Ca^{2+}]_i$ was paralleled by a decrease in apoptosis and explained by decreased activity of voltage-gated Ca^{2+} channels.

Finally, to prove that local islet production of apoCIII in vivo makes a difference for β-cell function and survival, on top of the already high systemic levels produced by the liver, we took advantage of a global apoCIII$^{-/-}$ mouse (30) and the ACE as an in vivo experimental platform (22). In this way, we could create a situation where the same animal served both as a control and a β-cell–specific apoCIII$^{-/-}$, which should be the ultimate experimental system circumventing for any unspecific or compensatory effects. Consequently, transplanting apoCIII$^{-/-}$ islets into one eye and control islets from ob/ob or B6 mice into the other eye of an ob/ob mouse or a HFD-treated mouse, thereby exposing both types of islets to the same high systemic apoCIII levels originating from the liver, enabled us to show that islets lacking local production of apoCIII were protected and maintained normal function compared with islets expressing the apolipoprotein. In the latter case, islets demonstrated not only unphysiological increases in $[Ca^{2+}]_i$ and apoptosis but also much higher in vivo proliferative activity, paralleled by an increase in vessel density, islet macrophages, and NAD(P)H:FAD ratio, as a marker of β-cell metabolism. These changes are typical of an inflammatory milieu provided by apoCIII released locally within the islet as a consequence of insulin resistance (34–36).

In the present study, we have demonstrated that apoCIII can serve as a link between insulin resistance and β-cell failure in T2DM. Preventing insulin resistance at the islet level is thus crucial to preserve β-cell mass, especially during the late phase of T2DM, where β cells are progressively lost. If results are confirmed in human islets from T2DM patients, local islet production of apoCIII may become a drugable target and thereby form the basis for a novel diabetes treatment regimen. It is of interest to note that there are human data from subjects with a genetic mutation in the apoCIII gene and thereby life-long reduced levels of apoCIII, demonstrating that these persons are overall healthier and have increased insulin sensitivity (11).

Materials and Methods

Animals and Islets. Age-matched ob/ob (Lep^{ob}/Lep^{ob}) and ob/lean (Lep^{ob}/Lep^{+}) on a C57BL/6J background were obtained from our own breeding colony at Karolinska Institutet. Mice used in experiments were genotyped, and they were between 4 and 44 wk of age. ApoCIII$^{-/-}$ mice were originally generated at The Jackson Laboratories. The C57BL/6 mice were purchased from Harlan laboratories. Animal care and experiments were carried out according to the Animal Experiment Ethics Committee at Karolinska Institutet and the A*STAR Institutional Animal Care and Use Committees (Protocol Number 140905) at Lee Kong Chian School of Medicine. Human islets were obtained within the Nordic Network for Islet Transplantation and were approved by the Regional Ethical Review Boards in Uppsala and Stockholm.

Pancreatic Islet Isolation. Animals were killed by cervical dislocation and the pancreas perfused with 3 mL of 1 mg/mL collagenase A (Roche) in HBSS (Sigma) buffer supplemented with 0.2% BSA and 25 mM Hepes. Pancreas was thereafter extracted and digested at 37 °C for 20 min. Islets were handpicked and were either immediately used for mRNA/protein analysis or were cultured overnight in RPMI medium 1640 supplemented with 10% (vol/vol) FCS, 2 mM glutamine, as well as 100 U/mL and 100 μg/mL of penicillin and streptomycin, respectively.

Dispersion of Pancreatic Islets Into Single Cells. Isolated islets were washed with HBSS without Ca^{2+} and Mg^{2+} and dispersed into single cells by incubation with Accutase in PBS containing 0.5 mM EDTA (Innovative Cell Technologies). Cells were sorted according to the protocol previously described (37).

Cell Culture. MIN6 cells, between passage 35 and 42, were cultured in DMEM containing 11.1 mM glucose and supplemented with 100 U/mL penicillin, 100 μg/mL streptomycin, 2 mM glutamine, 10% (vol/vol) FCS, and 75 μM β-mercaptoethanol at 5% (vol/vol) CO_2 and 37 °C. MIN6 cells were transfected using Lipofectamine (Invitrogen) with the control expression construct containing tdTomato or c-Myc–tagged mouse apoCIII construct for 24 h. All experiments were performed 48 h after transfection.

Biosensor Construction and Transduction of Islets. pENTR2A.RIP1.FoxO1GFP was generated by replacing the cDNA for EGFP in pENTR2A.RIP1.EGFP with that of FoxO1-GFP obtained from pEGFP.N1.hFOXO1 (38). IRES-3Tomato was generated by introducing a cDNA encoding three copies of the red fluorescent protein dTomato (39) downstream of the IRES sequence in pIRES (Clontech). The IRES-3Tomato cassette was then introduced into pENTR2A.

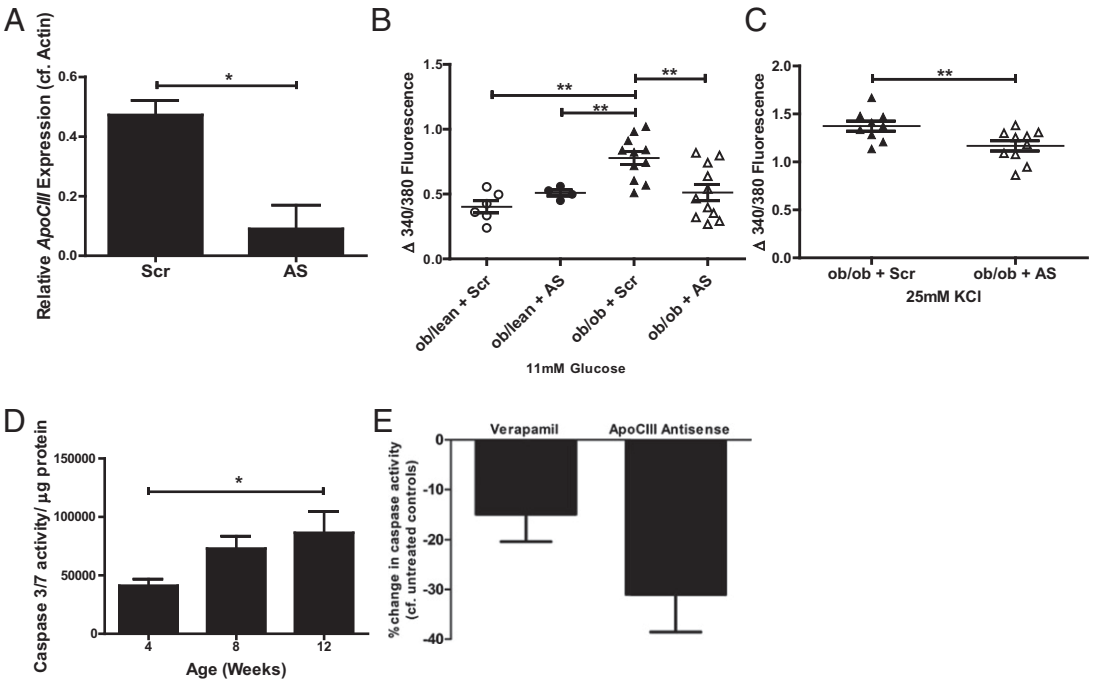

Fig. 4. Effects of decreasing apoCIII in ob/ob islets. (*A*) Isolated islets from 12-wk-old ob/ob mice exposed to apoCIII-specific (AS) or scr antisense oligonucleotides for 18 h. ApoCIII expression was measured by real-time qPCR to determine the efficacy of apoCIII knockdown in cultured islets ($n = 4$). (*B*) The ob/ob and ob/lean islets exposed to either active apoCIII or scr antisense were loaded with Fura-2AM and exposed to 11 mM glucose to determine glucose-stimulated Ca^{2+} influx ($n = 4$–11). (*C*) We used 25 mM KCl to induce depolarization and subsequent Ca^{2+} influx ($n = 9$–10). (*D*) Caspase 3/7 activity in ob/ob islets isolated from animals at 4, 8, and 12 wk of age ($n = 4$). (*E*) Decrease in caspase activity in β cells from 12-wk-old ob/ob mice either incubated overnight with the Ca^{2+}-channel blocker verapamil (left column) or exposed to apoCIII antisense (right column) ($n = 4$). $^*P < 0.05$, $^{**}P < 0.01$ by student's *t* test or ANOVA (Tukey's post hoc).

RIP1.FoxO1GFP, thus creating pENTR2A.RIP1.FoxO1GFP-IRES-3Tomato. pENTR2A.RIP1.FoxO1(H215R)GFP-IRES-3Tomato was generated by replacing histidine (CAT) 215 by arginine (CGT) by site-directed mutagenesis by using the QuikChange mutagenesis kit (Stratagene) and respective oligonucleotides purchased from Sigma. All constructions were verified by DNA sequencing. The expression cassette was transferred into the promoterless adenovirus plasmid pAd/PL-DEST (Invitrogen) by the Gateway technique. The ViraPower Adenoviral Expression System (Invitrogen) was used to generate a replication-deficient adenovirus, which was used for transduction of cells and islets. Islets from ob/lean and ob/ob mice were transduced with 10^7 pfu/mL of the biosensor encoding adenovirus.

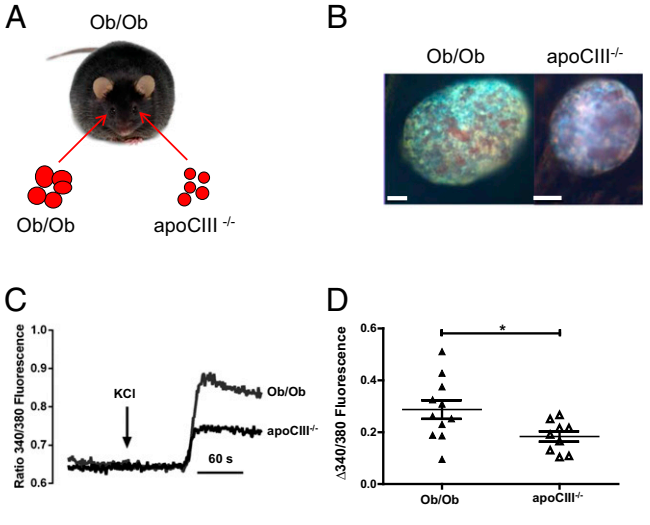

Fig. 5. The ob/ob and apoCIII$^{-/-}$ islets transplanted to the ACEs of ob/ob mice. (*A*) Islets from ob/ob and apoCIII$^{-/-}$ mice were transplanted into the right, respectively, and left ACE of 10-wk-old ob/ob mice. (*B*) Representative bright field images of islets from ob/ob (*Left*) and apoCIII$^{-/-}$ mice (*Right*). (Scale bar, 100 µm.) (*C*) Representative traces showing the effect of KCl on $[Ca^{2+}]_i$ in islets that have been microdissected out from the ACE of an ob/ob mouse with high levels of apoCIII 2 wk posttransplantation. (*D*) Increase in $[Ca^{2+}]_i$ when the islets are depolarized with KCl ($n = 11$ and 9, respectively). $^*P < 0.05$ by student's *t* test.

RNA Isolation and Quantitative RT-PCR Analysis. Total RNA was isolated from sorted cells or isolated pancreatic islets using the RNAeasy Micro Kit (Qiagen). Briefly, cells were lysed by first using RLT lysis buffer followed by a spin Qiashredder lysis. For liver and intestine RNA isolation, tissue/cell disruption was first carried out by a handheld rotor-stator homogenizer in RLT lysis buffer followed by 1,000 × *g* centrifugation for 5 min. The supernatant was subsequently transferred to a Qiashredder column to complete the lysis before the RNAeasy Mini Kit application (Qiagen). All lysates were applied to the RNAeasy spin column, and the subsequent RNA isolation and on-column DNase treatment were carried out according to manufacturer's recommendations. Total RNA was reverse transcribed at 37 °C with Multiscribe (Applied Biosystems). The expression of all genes was measured by real-time quantitative PCR with Taq SYBR Supermix with ROX (Invitrogen) on an ABI7900HT instrument (Applied Biosystems). β-actin was used as an endogenous control with one cycle at 95 °C for 10 min followed by 40 cycles of tandem 95 °C for 30 s and 60 °C for 1 min. Samples with poor RNA quality or yield (i.e., high actin Ct) were excluded from analysis. In all cases, unless otherwise stated, gene-specific intron spanning primers were used, and the PCR melting curve produced one single peak corresponding to a specific single amplified product.

Metabolic Studies. Nonfasted glucose was measured with a glucose meter (Accu-Chek Advantage, Roche Diagnostics) and serum insulin by the ArcDia 2-photon fluorescence excitation microparticle fluorometry (TPX) assay for insulin (ArcDia Group). An i.p. glucose tolerance test (IPGTT) was performed in mice fasted for 6 or 12 h. Blood glucose was measured at 0, 15, 30, 45, 60, 90, and 120 min after an i.p. glucose injection of 2 g/kg body weight. C57BL/6 mice (Harlan Laboratories) were fed a HFD (Open Source Diets D12492, Research Diets Inc.) consisting of 60% kcal from fat from the age of 4–9 mo.

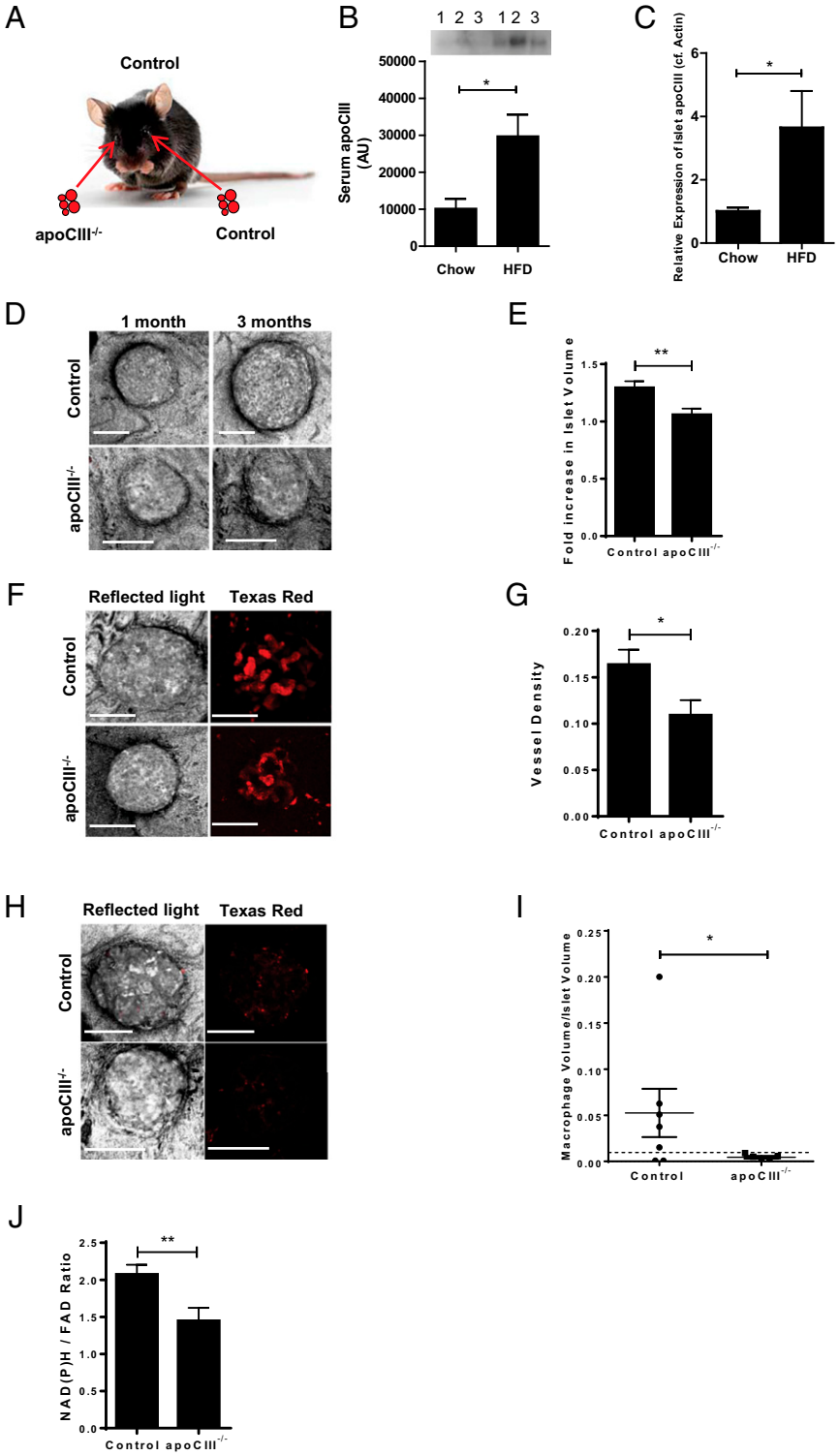

Fig. 6. Local islet production of apoCIII affects islet growth and macrophage infiltration in vivo independent of high systemic levels of apoCIII. (*A*) Islets from apoCIII$^{-/-}$ and B6 mice were transplanted into the right, respectively, and left ACE of B6 mice ($n = 6$). (*B*) Western blot analysis and quantitation of the band intensities of serum apoCIII from B6 mice fed normal chow (control) or HFD ($n = 3$). (*C*) Expression of apoCIII in islets from B6 mice fed normal chow (control) or HFD ($n = 5$). (*D*) The recipient mice were fed a HFD, and the transplanted islets were imaged from 1 to 3 mo posttransplantation. (Scale bar, 100 μM.) (*E*) Fold increase in islet area from 1 to 3 mo posttransplantation ($n = 8$). (*F*) Texas Red-labeled dextran was injected to visualize blood vessels. (*G*) The vessel density (vessel volume/islet volume) was calculated ($n = 8$). (*H*) Infiltration of macrophages was evaluated 72 h after injection of Texas Red-labeled dextran. Remnants of the labeled dextran were phagocytized by macrophages that can be observed in red to the right. (*I*) The volume of macrophages in relation to volume of the transplanted islets. (*J*) The NAD(P)H:FAD ratio was calculated as a measure of mitochondrial metabolism ($n = 4$). *$P < 0.05$ by student's *t* test (*B*, *E*, *G*, and *J*), Mann–Whitney *U* test (*C*), or Fisher's exact test (*I*).

Western Blotting. Islets or cells were washed with PBS, lysed with RIPA buffer (50 mM Tris pH 7.5, 150 mM NaCl, 1% Nonidet P-40, 0.5% Na deoxycholate, 0.1% SDS, EDTA-free protease inhibitor mixture, and 1 μg/mL pepstatine and leupeptin). Lysates were passed five times through a syringe needle (0.33 × 13 mm/29 Gx1/2) followed by 30 min of incubation on a rotator at 4 °C. Homogenates were spun at 10,000 × *g* for 10 min, and the protein amount was determined in the supernatants by the BCA method (Thermo Scientific Pierce). Equal amounts of protein (25–50 μg) were separated over a 4–12% Bis–Tris gel with Mes buffering system (Invitrogen). Proteins were subsequently electrotransferred to PVDF membrane. In case of the phosphospecific antibodies, the membranes were probed with the respective antibodies and then stripped and reprobed with antibodies recognizing the respective total protein levels. Rabbit anti-FoxO1, rabbit anti–phospho-FoxO1, Akt, and phospho-Akt antibodies were purchased from Cell Signaling Technology (Danvers). Further antibodies used were rabbit anti-apoCIII antibody (Santa Cruz), guinea-pig c-peptide (Abcam), mouse anti-cMyc (Santa Cruz), and mouse anti-tubulin (Abcam). Immunoreactivity was detected with horseradish peroxidase-conjugated secondary antibodies using the ECL system (Amersham). For immunoblotting serum apoCIII, after serum collection (50 μL) per animal, samples were albumin-depleted and freeze-dried. Samples were then resuspended in RIPA buffer (50 μL), and protein amount was determined by BCA method (Thermo Scientific Pierce). Equal amounts of protein (25 μg) were separated over a 4–12% Bis–Tris gel with Mes buffering system (Invitrogen) as described above. Ponceau S [0.1% (wt/vol)] in 1% (vol/vol) acetic acid was used to stain transferred proteins on PVDF blots before blocking. After 5 min, blots were rinsed with 5% (vol/vol) acetic acid with gentle agitation, followed by three washes in de-ionized water to allow for visualization of protein bands.

Immunocytochemistry. To visualize Myc-tagged apoCIII in MIN6 cells, post-transfected cells were cultured on glass coverslips before 3% (vol/vol) PFA fixation for 30 min. Subsequently, cells were incubated with antibodies specific for c-Myc (mouse monoclonal, Santa-Cruz) and C-peptide (rabbit polyclonal, Cell Signaling) in 10% (vol/vol) goat serum blocking buffer containing 0.25% Triton X-100, overnight at 4 °C with gentle shaking. Cells were incubated with Alexa 488 anti-mouse (Santa Cruz) and Alexa 546 anti-rabbit (Cell Signaling) in blocking buffer for 1 h followed by washing and mounting using VectaShield mounting media with DAPI (Vector Labs). Freshly isolated islets were fixed with 4% (vol/vol) PFA in PBS for at least 48 h. They were incubated with primary antibodies anti-FoxO1 (rabbit monoclonal, Cell Signaling) and anti-insulin (guinea pig, DAKO/Agilent) in the presence of 0.1% Triton X-100 for permeabilization and 2% (vol/vol) BSA for blocking for 48 h at room temperature. Islets were then washed three times with PBS and incubated with the secondary antibodies Alexa 488-labeled anti-rabbit and Alexa 633-labeled anti-guinea pig (Life Technologies) in the presence of 0.1% Triton X-100 and 2% (vol/vol) BSA. Human islets were fixed for 30 min in 4% (vol/vol) PFA and thereafter incubated overnight at 4 °C with primary antibodies anti-insulin (guinea pig, DAKO/Agilent) and anti-apoCIII (Santa Cruz), in 10% (vol/vol) goat serum blocking buffer containing 0.25% Triton X-100. After washing, the islets were incubated with the secondary antibodies Alexa 488-labeled anti-guinea pig and Alexa 647 anti-rabbit (Life Technologies). The islets were imaged by confocal laser scanning microscopy.

In Vivo Treatment with Antisense to ApoCIII. Ob/ob (Lep^{ob}/Lep^{ob}) mice were treated with apoCIII antisense (ISIS 353982) or an inactive control (ISIS 141923) ($n = 6$ per group). We i.p. administered 25 mg/kg body weight twice per week between the ages of 8 and 16 wk.

Intraocular Islet Transplantation. Isolated islets from ob/ob, $apoCIII^{-/-}$, and C57BL/6 mice were transplanted into the ACE of ob/ob ($n = 8$) or C57Bl6 ($n = 8$) mice as described previously (22). Biosensor-transduced islets from ob/lean and ob/ob mice were transplanted into the ACE of 8-wk-old syngeneic littermate recipients.

In Vivo and in Vitro Imaging of Islets and Image Analysis. The islet grafts were imaged in vivo as previously described (22) using a TCS-SP5 II laser scanning confocal microscope (Leica Microsystems) with water-dipping objectives (Leica HCX IRAPO L 25.0 × 0.95 and HXC-APO10×/0.30 NA). Viscotears (Novartis) was used as the immersion liquid between the eye and the objective. The mice were anesthetized with Isoflurane (Baxter). Bright field images of islet grafts were obtained by the DFC 295 digital camera (Leica Microsystems). To visualize blood vessels and macrophages, 100 μL of 2.5 ng/μL of Texas red-labeled Dextran (Life Technologies) was injected into the tail vein. Vessel density was calculated by normalizing the vessel volume to the islet volume. Blood vessels were imaged directly after injection, whereas macrophages were imaged 72 h later.

Islet autofluorescence from NAD(P)H and FAD was determined by 2-photon laser-scanning microscopy using the same microscope setup as described above, but without loading with the indicator (40). The redox ratio NAD(P)H:FAD was calculated using LAS AF software (Leica Microsystems). Excitation wavelengths were 760 nm for NAD(P)H and 900 nm for FAD. Fluorescence was detected after band-pass filters 460/50 and 525/50 for NAD(P)H and FAD, respectively. In the transduced islets, GFP fluorescence was excited at a 488 nm and fluorescence detected at 505–536 nm. Tomato was excited at 561 nm and fluorescence detected at 580–650 nm. Backscatter signal from the 561 nm excitation was collected at 555–565 nm. Imaging of immunostained mouse islets was performed with an inverted Leica TCS-SP2 with a PL APO CS 20×/0.7 NA objective and of human islets with TCS-SP5 II laser scanning confocal microscope (Leica Microsystems) with a water-dipping objective (Leica HCX IRAPO L 25.0 × 0.95).

Analyses of islet volume, vessel volume, and macrophage infiltration were performed with Volocity image analysis software (Perkin-Elmer). Vessel density was calculated by normalizing the vessel volume to the islet volume. Image analyses of transduced cells and islets were performed using LAS AF software. For each cell the central plane was determined using information from each detection channel (GFP, Tomato, backscatter). Three regions of interest were drawn manually for each cell—namely, nucleus, cytoplasm, and background, respectively. Information from all three detection channels was used to determine the position of the nucleus. To calculate the nuclear:cytoplasm ratio, only the intensity values of the GFP channel were considered. The ratio for each cell was calculated as follows: ratio = (nucleus – background) / (cytoplasm – background). The ratios were categorized into two groups: (*i*) Ratios <1 were considered nuclear FoxO1GFP(HR) negative, as less signal was found in the nucleus than in the cytoplasm. (*ii*) Ratios ≥1 were considered nuclear FoxO1GFP(HR) positive, as more (or at least equal) signal was found in the nucleus than in the cytoplasm. For each experiment in vitro or in vivo, the percentage of nuclear FoxO1GFP(HR) positive cells was calculated as follows: nuclearFoxO1GFP(HR) (%) = cells with a ratio ≥1 / total amount of analyzed cells.

Measurements of $[Ca^{2+}]_i$. Changes in $[Ca^{2+}]_i$ were recorded in islets after a 16-h incubation period with 0.07 mg/mL apoCIII antisense or a scrambled control (Isis Pharmaceuticals) in RPMI medium 1640 and in islets immediately after microdissection from ACE 2 wk posttransplantation. The basal medium used for islet perifusion experiments was a Hepes buffer (pH 7.4), containing 125 mM NaCl, 5.9 mM KCl, 2.6 mM $CaCl_2$, 1.2 mM $MgCl_2$, and 25 mM Hepes, 0.1% BSA supplemented with either 3 mM glucose, 11 mM glucose, or 25 mM KCl. Islets, loaded with 2 μM Fura-2AM (Molecular Probes), were attached to coverslips using Puramatrix Hydrogel (BD Biosystem) and mounted on an inverted epifluorescence microscope (Zeiss, Axiovert 135) connected to a Spex Industries Fluorolog system for dual-wavelength excitation fluorimetry. The measurements were performed as previously described (33).

Caspase Assay. Activity of capase 3/7 was determined using SensoLyte Homogeneous Rh110 Caspase 3/7 assay kit according to the manufacturer's instructions, with modifications (AnaChem). Briefly, islets or cells were harvested, lysed using lysis buffer (AnaChem), and the protein quantified using BCA method. We loaded 10 μg of protein in a black 384-well plate and topped it up with the appropriate amount of assay buffer (AnaChem) containing Rh110 Caspase 3/7 substrate. Plate was incubated in the dark for 1 h at 24 °C. Fluorescence intensity at Ex/Em = 490/520 nm was measured to determine the relative caspase activity.

Statistical Analysis. For individual experiments, the number of animals or islets used (*n*) is included in each figure legend in parentheses. All results are expressed as mean ± SEM. Statistical analyses were performed with GraphPad Prism 5, IBM SPSS Statistics 22, and Microsoft Excel 2007. A Student's *t* test, one-way ANOVA (Tukey's post hoc), or Mann–Whitney *U* test were used when appropriate. *P* values <0.05 were considered statistically significant. In Fig. 6*E* a Fisher's exact test was performed.

ACKNOWLEDGMENTS. This work was supported by the Swedish Diabetes Association; Funds of Karolinska Institutet; The Swedish Research Council; Novo Nordisk Foundation; The Family Erling-Persson Foundation; Strategic Research Program in Diabetes at Karolinska Institutet; The ERC-2013-AdG 338936-BetaImage; The Family Knut and Alice Wallenberg Foundation; Skandia Insurance Company; Diabetes and Wellness Foundation; The Bert von Kantzow Foundation; Svenska Diabetesstiftelsen; Lee Kong Chian School of Medicine, Nanyang Technological University Start-Up Grant (separately for Y.A. and P.-O.B.); The Stichting af Jochnick Foundation; and Diabetes Research Institute Foundation. Y.A. was supported in part by the Agency for Science, Technology and Research, in Singapore. Human islets were provided through Juvenile Diabetes Research Foundation (JDRF) Award 31-2008-416 [European Consortium for Islet Transplantation (ECIT) Islet for Basic Research program].

1. Butler AE, et al. (2003) Beta-cell deficit and increased beta-cell apoptosis in humans with type 2 diabetes. *Diabetes* 52(1):102–110.
2. Sakuraba H, et al. (2002) Reduced beta-cell mass and expression of oxidative stress-related DNA damage in the islet of Japanese Type II diabetic patients. *Diabetologia* 45(1):85–96.
3. Ginsberg HN, et al. (1986) Apolipoprotein B metabolism in subjects with deficiency of apolipoproteins CIII and AI. Evidence that apolipoprotein CIII inhibits catabolism of triglyceride-rich lipoproteins by lipoprotein lipase in vivo. *J Clin Invest* 78(5): 1287–1295.
4. Krauss RM, Herbert PN, Levy RI, Fredrickson DS (1973) Further observations on the activation and inhibition of lipoprotein lipase by apolipoproteins. *Circ Res* 33(4): 403–411.
5. Altomonte J, et al. (2004) Foxo1 mediates insulin action on apoC-III and triglyceride metabolism. *J Clin Invest* 114(10):1493–1503.
6. Chen M, Breslow JL, Li W, Leff T (1994) Transcriptional regulation of the apoC-III gene by insulin in diabetic mice: Correlation with changes in plasma triglyceride levels. *J Lipid Res* 35(11):1918–1924.
7. Caron S, et al. (2011) Transcriptional activation of apolipoprotein CIII expression by glucose may contribute to diabetic dyslipidemia. *Arterioscler Thromb Vasc Biol* 31(3): 513–519.
8. Salerno AG, et al. (2007) Overexpression of apolipoprotein CIII increases and CETP reverses diet-induced obesity in transgenic mice. *Int J Obes (Lond)* 31(10):1586–1595.
9. Chan DC, Nguyen MN, Watts GF, Barrett PH (2008) Plasma apolipoprotein C-III transport in centrally obese men: Associations with very low-density lipoprotein apolipoprotein B and high-density lipoprotein apolipoprotein A-I metabolism. *J Clin Endocrinol Metab* 93(2):557–564.
10. Petersen KF, et al. (2010) Apolipoprotein C3 gene variants in nonalcoholic fatty liver disease. *N Engl J Med* 362(12):1082–1089.
11. Atzmon G, et al. (2006) Lipoprotein genotype and conserved pathway for exceptional longevity in humans. *PLoS Biol* 4(4):e113.
12. Pollin TI, et al. (2008) A null mutation in human APOC3 confers a favorable plasma lipid profile and apparent cardioprotection. *Science* 322(5908):1702–1705.
13. Jørgensen AB, Frikke-Schmidt R, Nordestgaard BG, Tybjærg-Hansen A (2014) Loss-of-function mutations in APOC3 and risk of ischemic vascular disease. *N Engl J Med* 371(1):32–41.
14. Coleman DL, Hummel KP (1973) The influence of genetic background on the expression of the obese (Ob) gene in the mouse. *Diabetologia* 9(4):287–293.
15. Kaneko K, et al. (2010) Class IA phosphatidylinositol 3-kinase in pancreatic β cells controls insulin secretion by multiple mechanisms. *Cell Metab* 12(6):619–632.
16. Leibiger B, et al. (2010) Insulin-feedback via PI3K-C2alpha activated PKBalpha/Akt1 is required for glucose-stimulated insulin secretion. *FASEB J* 24(6):1824–1837.
17. Kerouz NJ, Hörsch D, Pons S, Kahn CR (1997) Differential regulation of insulin receptor substrates-1 and -2 (IRS-1 and IRS-2) and phosphatidylinositol 3-kinase isoforms in liver and muscle of the obese diabetic (ob/ob) mouse. *J Clin Invest* 100(12): 3164–3172.
18. Zawalich WS, Tesz GJ, Zawalich KC (2002) Inhibitors of phosphatidylinositol 3-kinase amplify insulin release from islets of lean but not obese mice. *J Endocrinol* 174(2): 247–258.
19. Kitamura T, et al. (2002) The forkhead transcription factor Foxo1 links insulin signaling to Pdx1 regulation of pancreatic beta cell growth. *J Clin Invest* 110(12): 1839–1847.
20. Kitamura YI, et al. (2005) FoxO1 protects against pancreatic beta cell failure through NeuroD and MafA induction. *Cell Metab* 2(3):153–163.
21. Okamoto H, et al. (2006) Role of the forkhead protein FoxO1 in beta cell compensation to insulin resistance. *J Clin Invest* 116(3):775–782.
22. Speier S, et al. (2008) Noninvasive high-resolution in vivo imaging of cell biology in the anterior chamber of the mouse eye. *Nat Protoc* 3(8):1278–1286.
23. Kamagate A, et al. (2008) FoxO1 mediates insulin-dependent regulation of hepatic VLDL production in mice. *J Clin Invest* 118(6):2347–2364.
24. Sol EM, Sundsten T, Bergsten P (2009) Role of MAPK in apolipoprotein CIII-induced apoptosis in INS-1E cells. *Lipids Health Dis* 8:3.
25. Holmberg R, et al. (2011) Lowering apolipoprotein CIII delays onset of type 1 diabetes. *Proc Natl Acad Sci USA* 108(26):10685–10689.
26. Juntti-Berggren L, et al. (2004) Apolipoprotein CIII promotes Ca2+-dependent beta cell death in type 1 diabetes. *Proc Natl Acad Sci USA* 101(27):10090–10094.
27. Li X, Grundy SM, Patel SB (1997) Obesity in db and ob animals leads to impaired hepatic very low density lipoprotein secretion and differential secretion of apolipoprotein B-48 and B-100. *J Lipid Res* 38(7):1277–1288.
28. Kluth O, et al. (2011) Dissociation of lipotoxicity and glucotoxicity in a mouse model of obesity associated diabetes: Role of forkhead box O1 (FOXO1) in glucose-induced beta cell failure. *Diabetologia* 54(3):605–616.
29. Shi Y, et al. (2014) Apolipoprotein CIII hyperactivates β cell CaV1 channels through SR-BI/β1 integrin-dependent coactivation of PKA and Src. *Cell Mol Life Sci* 71(7): 1289–1303.
30. Duivenvoorden I, et al. (2005) Apolipoprotein C3 deficiency results in diet-induced obesity and aggravated insulin resistance in mice. *Diabetes* 54(3):664–671.
31. Prentki M, Nolan CJ (2006) Islet beta cell failure in type 2 diabetes. *J Clin Invest* 116(7): 1802–1812.
32. Kulkarni RN, et al. (1999) Tissue-specific knockout of the insulin receptor in pancreatic beta cells creates an insulin secretory defect similar to that in type 2 diabetes. *Cell* 96(3):329–339.
33. Refai E, et al. (2005) Transthyretin constitutes a functional component in pancreatic beta-cell stimulus-secretion coupling. *Proc Natl Acad Sci USA* 102(47):17020–17025.
34. Dirice E, et al. (2014) Soluble factors secreted by T cells promote β-cell proliferation. *Diabetes* 63(1):188–202.
35. Mezza T, et al. (2014) Insulin resistance alters islet morphology in nondiabetic humans. *Diabetes* 63(3):994–1007.
36. Miska J, et al. (2014) Real-time immune cell interactions in target tissue during autoimmune-induced damage and graft tolerance. *J Exp Med* 211(3):441–456.
37. Köhler M, et al. (2012) One-step purification of functional human and rat pancreatic alpha cells. *Integr Biol (Camb)* 4(2):209–219.
38. Zhao X, et al. (2004) Multiple elements regulate nuclear/cytoplasmic shuttling of FOXO1: Characterization of phosphorylation- and 14-3-3-dependent and -independent mechanisms. *Biochem J* 378(Pt 3):839–849.
39. Shaner NC, et al. (2004) Improved monomeric red, orange and yellow fluorescent proteins derived from Discosoma sp. red fluorescent protein. *Nat Biotechnol* 22(12): 1567–1572.
40. Skala M, Ramanujam N (2010) Multiphoton redox ratio imaging for metabolic monitoring in vivo. *Methods Mol Biol* 594:155–162.